epigenomes

MDPI

Article

Large-Scale Integrative Analysis of Epigenetic Modifications Induced by Isotretinoin, Doxycycline and Metronidazole in Murine Colonic Intestinal Epithelial Cells

Eugenia Becker [1], Susan Bengs [1], Sirisha Aluri [2], Lennart Opitz [2], Kirstin Atrott [1], Felix Rost [3] , Irina Leonardi [1] , Claudia Stanzel [1], Tina Raselli [1], Stephanie Kasper [1], Pedro A. Ruiz [1] and Gerhard Rogler [1,*]

[1] Division of Gastroenterology and Hepatology, University Hospital Zurich, Rämistrasse 100, CH-8091 Zurich, Switzerland; Eugenia.becker@usz.ch (E.B.); Susan.bengs@usz.ch (S.B.); Kirstin.atrott@usz.ch (K.A.); Irina.leonardi@gmail.com (I.L.); Claudia.stanzel@gmx.at (C.S.); Tina.raselli@usz.ch (T.R.); Kasper.stephanie@googlemail.com (S.K.); PedroAntonio.Ruiz-Castro@usz.ch (P.A.R.)
[2] Functional Genomics Center Zurich, ETH/University of Zurich, Winterthurerstrasse 190, 8057 Zurich, Switzerland; Sirisha.aluri@fgcz.ethz.ch (S.A.); Lennart.opitz@fgcz.uzh.ch (L.O.)
[3] Institute of Experimental Immunology, University of Zurich, Winterthurerstrasse 190, 8057 Zurich, Switzerland; Rost@immunology.uzh.ch
* Correspondence: gerhard.rogler@usz.ch; Tel.: +41-(0)44-255-9477; Fax: +41-(0)44-255-9497

Abstract: Environmental factors are playing a central role in triggering inflammatory responses in the intestine. There is increasing evidence that the development of inflammatory bowel disease (IBD) is deriving from an aberrant immune response to the commensal gut microbiota triggered by various environmental factors in a susceptible host. A vitamin A derivate used in acne therapy (isotretinoin) has been inconsistently associated with the onset of IBD. However, what needs to be considered is the previous treatment of acne patients with antibiotics that are also associated with the development of IBD, thus representing a crucial confounding factor. Here, we studied whether doxycycline (acne therapy), metronidazole (IBD therapy) or isotretinoin are able to induce alterations in DNA methylation and microRNA expression patterns in murine colonic intestinal epithelial cells (IECs). Additionally, we analyzed time-dependent changes in the aforementioned epigenetic mechanisms to study how epigenetic signatures evolve over time. As for changes in DNA methylation, we found isotretinoin to have strong demethylating effects, while antibiotic treatment had only a moderate impact. Isotretinoin-mediated demethylation resolved after a washout phase, not supporting an association between isotretinoin treatment and IBD. Regarding microRNA and mRNA expression, isotretinoin and doxycycline, but not metronidazole, potentially induce long-term changes in microRNA/mRNA expression profiles towards the down-regulation of immune responses. Analysis of time-dependent DNA methylation showed stable marks over a time frame of 4 weeks. Furthermore, novel microRNAs were identified (e.g., microRNA-877-3p), which might be of relevance in IEC development.

Keywords: DNA methylation; microRNA expression; intestinal epithelial cells; antibiotics; isotretinoin; IBD

1. Introduction

Intestinal epithelial cells (IECs) form a specialized monolayer representing the first line of contact with the luminal content and thus an essential component of the intestinal barrier function protecting the body integrity. Disruption of the intestinal epithelial barrier is an important event in the pathogenesis of inflammatory bowel diseases (IBDs). The two predominant forms of IBD, Crohn's disease (CD) and ulcerative colitis (UC), are both chronic and relapsing inflammatory conditions of the gastrointestinal tract with increasing incidences worldwide [1]. The multifactorial pathogenesis of IBD is not yet completely understood, but it is generally considered that environmental factors and the gut microbiome combined with the genetic susceptibility represent a complex interplay that determines the onset and progression of IBD [2].

Mounting evidence supports the concept that IBD is a polygenic disease and that not only genetic but also epigenetic modifications might have an impact on its susceptibility and severity [3]. Mechanisms of transcriptional regulation that do not alter the sequence of DNA are called epigenetic regulations and have been studied extensively over the last few years. These studies have shown that epigenetics play a relevant role in a variety of diseases, e.g., IBD [4,5], multiple sclerosis [6], psoriasis [7] and systemic lupus erythematosus (SLE) [8]. Importantly, epigenetic marks may persist through cell division and are inheritable to next generations (long-term effects) [9]. There are currently three major epigenetic modifications that have been identified: DNA methylation, histone and nucleosome modifications and differential microRNA expression.

DNA methylation is the most extensively studied epigenetic modification occurring at the pyrimidine ring of cytosine at CpG dinucleotide sequences. In general, highly methylated CpGs (hypermethylation) are associated with silencing of the respective gene. Lower methylated sites (hypomethylation) are loosely arranged and harbor active histone marks, such as H3K4me3, and H3K9ac that enable transcriptional protein complexes to bind to the DNA [10–12]. Another well studied epigenetic modification is the expression of microRNAs, which are associated with translational silencing. MicroRNAs are small non-coding RNA molecules of 18–24 nucleotides. Via the RNA-induced silencing complex (RISC) the microRNAs are able to bind to complementary regions in the 3′ untranslated region (3′-UTR) of their target mRNAs. This specific interaction leads to sequestration, degradation or storage of the target mRNA [13].

Several epidemiological reports have suggested a potential association between isotretinoin, a vitamin A derivate prescribed against severe acne, and the development of IBD. In case reports, intestinal inflammation was observed during medication, immediately or several weeks or months after the last drug administration [14–16]. Yet, these results remain controversial as others were unable to confirm these findings in epidemiological studies [17–19]. Moreover, in vitro and in vivo studies have shown evidence against an association between isotretinoin and IBD, and demonstrated that isotretinoin induces anti-inflammatory effects [20,21]. Isotretinoin is typically used in acne patients unresponsive to antibiotic therapy [22,23]. A growing body of literature indicates that antibiotics can impact on the incidence of IBD and increase the risk of IBD development in children and adults, pointing to long-term effects after antibiotic therapy [22,24–27]. Thus, any attempt to confirm a causal association between isotretinoin and IBD is confounded by prior antibiotic treatment [28].

Here, we analyzed alterations in the DNA methylation, as well as microRNA and mRNA expression in murine IECs ex vivo to elucidate the epigenome-modifying properties of isotretinoin, and the antibiotics doxycycline (applied in acne therapy and associated with IBD), and metronidazole (preferred antibiotic in IBD therapy). Additionally, we have investigated time-dependent epigenetic marks in IECs to evaluate how the epigenetic signature evolves over time. To analyze drug- and time-dependent effects, samples were collected straight after a 2-week oral treatment, and 4 weeks after the last drug administration. The latter time point is henceforth referred to as the washout phase.

2. Results

To elucidate direct and long-term drug-induced changes, as well as time-dependent alterations in murine colonic IECs upon oral administration of isotretinoin, metronidazole, doxycycline or vehicles (Figure 1), we assessed changes in DNA methylation and microRNA expression along with changes at the transcriptome level at two different time points using next generation sequencing. Studying epigenetic modifications in IECs allowed us to determine potential protective or harmful immunomodulatory changes induced by the three agents that might have an impact on IBD development right after the end of treatment or later on. Additionally, our experimental setting enabled us to study epigenetic signatures evolving over time that might be crucial in IEC development.
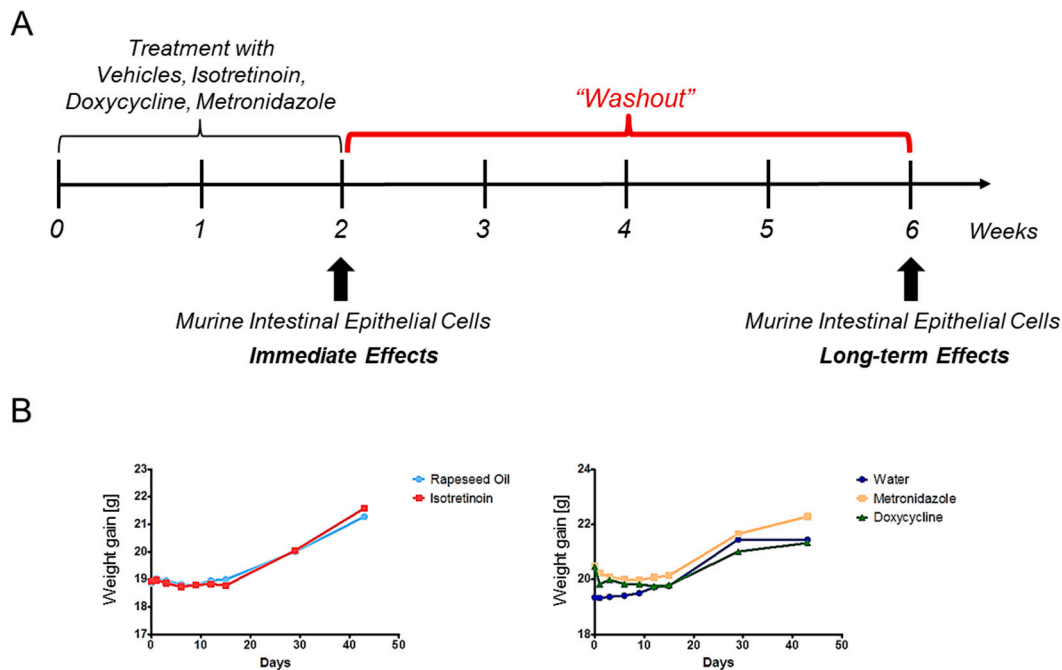

Figure 1. Experimental design. BALB/c female mice were treated with isotretinoin, seed oil (vehicle of isotretinoin), metronidazole, doxycycline or water (vehicle for both antibiotics) by daily per os treatment for 2 weeks. (**A**) Intestinal epithelial cells (IECs) were harvested after 2 weeks (immediate effects) and 4 weeks after last dose administration, referred to as the washout phase (long-term effects). For all animal groups, a replicate number of six animals were collected per time point and group and individually processed without pooling. (**B**) No differences between treatment groups were observed with respect to body weight until the end of the study. Reproduced with permission from Eugenia Becker; Doxycycline, metronidazole and isotretinoin: Do they modify microRNA/mRNA expression profiles and function in murine T-cells? Published by Scientific Reports, 2017 [28].

2.1. Quantitative Overview of Epigenetic Modifications after Treatment Courses per Time Point

All three orally administered agents induced changes in the methylation status applying the following thresholds |log2 (fold change)| $\geq$ 1, *p*-value $\leq$ 0.001. Figure 2A depicts the number of significantly hypermethylated or hypomethylated targets per treatment and time point. The 5-aza-2-deoxycytidine (DAC) treated group served as a positive control to rank the potential to induce changes in the global DNA methylation status. DAC is a potent DNA methyltransferase (DNMT) inhibitor by irreversible binding DNMTs, thereby leading to an inhibition of DNA methylation and relaxation of the chromatin structure. Treatment with DAC resulted in 550 hypomethylated and 184 hypermethylated targets. The latter finding might occur due to the high proliferative properties of the intestine and the used DAC treatment regime, so a partial restoration of DNA methylation was observed.
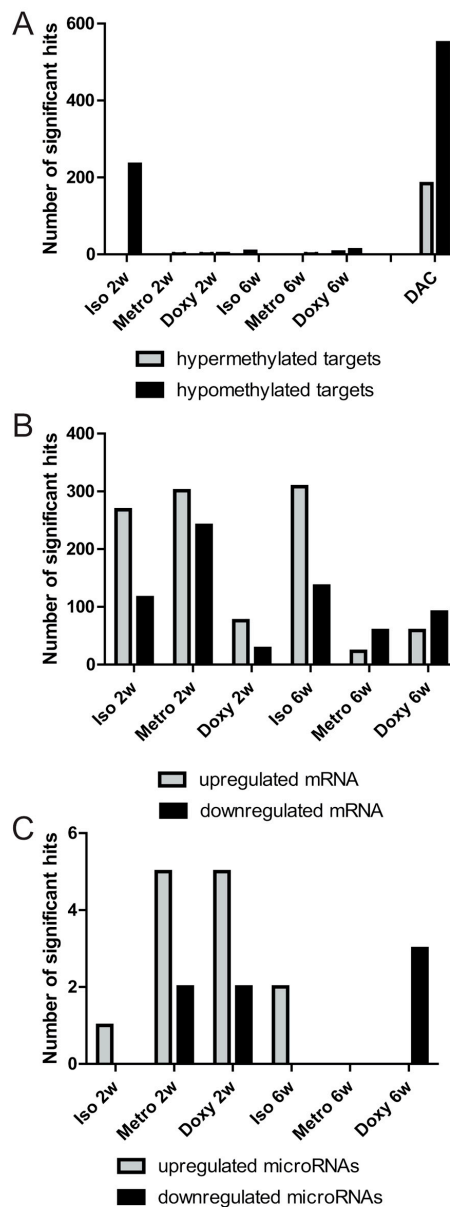
Figure 2. Quantitative analysis of drug-induced effects on epigenetic mechanisms. (**A**) Changes at the DNA methylation level directly after treatment cessation and after the washout phase of individually treated animals. Selection of differentially methylated targets was performed with the following thresholds: |log2 (fold change)| ≥ 1, *p*-value ≤ 0.001. 5-Aza-2-deoxycytidine (DAC) is a potent DNA demethylating agent and serves as a positive control. (**B**) Alterations of differentially expressed mRNAs per time point and treatment regime. Selection of differentially expressed mRNAs was done with the thresholds: |log2 (fold change)| ≥ 0.5, *p*-value ≤ 0.05. (**C**) Number of significantly modified microRNAs per time point and treatment regime. Selection of differentially expressed microRNAs was performed with thresholds |log2 (fold change)| ≥ 1, *p*-value ≤ 0.001. Iso = Isotretinoin, Metro = Metronidazole, Doxy = Doxycycline.

Directly after, antibiotic treatment induced only minor changes in the patterns of DNA methylation. Upon treatment with doxycycline, 1 hypermethylated target (*LOC100041346*) and 2 hypomethylated targets (*Vmn2r40*, *Esam*) were found, while only 1 hypomethylated target (*Kcnt2*) was identified upon treatment with metronidazole. In contrast, isotretinoin had a strong impact on DNA methylation with 234 hypomethylated targets compared to the vehicle. After the washout phase, we identified six hypermethylated and twelve hypomethylated targets upon

treatment with doxycycline, whereas only one hypomethylated target (*Lmx1a*) was found upon metronidazole-treatment. Previous treatment with isotretinoin resulted in eight hypermethylated targets, indicating a resolution of the direct effect on demethylation, and thereby pointing to a short-term effect of isotretinoin on DNA methylation.

We observed a different mRNA expression pattern with more differentially expressed mRNAs in the isotretinoin and metronidazole groups directly after the treatment period, while the effects of doxycycline were limited, with only 76 and 28 mRNAs up- or down-regulated, respectively (Figure 2B). Long-term effects differed between isotretinoin and the antibiotic treated groups. In total, 308 mRNAs were up-regulated and 136 mRNAs down-regulated after isotretinoin-washout, while treatment with metronidazole and doxycycline up-regulated the expression of 23 and 59 mRNAs, respectively, and down-regulated the expression of 59 and 91 mRNAs, respectively. These results point to possible long-term changes on mRNA expression levels after isotretinoin treatment in murine colonic IECs.

In the analysis of predicted microRNA targets (Figure 2C), metronidazole and doxycycline potentially induced 960 and 1029 microRNA targets, and suppressed 11,034 and 10,465 microRNA targets, respectively, after cessation of treatment. In comparison, isotretinoin induced the expression of only one microRNA (microRNA-451a) directly after the treatment period. After the washout phase, doxycycline suppressed the expression of three microRNAs (Table 1A), thereby inducing 3517 potential microRNA targets, whereas metronidazole led to no changes in microRNA expression after the washout phase. Isotretinoin led to an increase in the expression of two microRNAs (microRNA-98-3p, -142b) after the washout phase, pointing to the inhibition of 9156 predicted microRNA targets.

Table 1. Drug- and time-dependent alterations of differentially expressed microRNAs in IECs. (**A**) Changes of microRNA expression after isotretinoin, doxycycline and metronidazole directly after treatment cessation and after the respective washout phases. Selection of significantly regulated microRNAs was done with: $|\log2\ (\text{fold change})| \geq 1$, *p*-value ≤ 0.001. Numbers of significantly modified microRNA targets by inversely expressed microRNAs per time point and treatment regime were predicted by TargetScan and TargetScan custom [29,30]. (**B**) Changes of microRNA expression over time of water or seed oil treated animals. FC = fold change; mmu = mus musculus; miR = microRNA.

A

Treatment vs. Vehicles per Time Point	Regulation	microRNA	Log2FC	*p*-Value	In silico microRNA targets
Isotretinoin 2 weeks	Induction	mmu-miR-451a	1.361	4.03×10^{-4}	24↓
Isotretinoin 6 weeks	Induction	mmu-miR-98-3p	2.078	2.65×10^{-5}	5326↓
		mmu-miR-142b	1.805	1.99×10^{-4}	3830↓
Metronidazole 2 weeks	Induction	mmu-miR-19b-3p	1.2	5.72×10^{-6}	1075↓
		mmu-miR-1983	1.719	1.05×10^{-5}	4154↓
		mmu-miR-219a-5p	1.599	1.16×10^{-5}	388↓
		mmu-miR-19a-3p	1.295	3.25×10^{-5}	1075↓
		mmu-miR-219c-3p	1.387	7.97×10^{-5}	4342↓
	Suppression	mmu-miR-1247-5p	−1.356	1.76×10^{-4}	909↑
		mmu-miR-409-5p	−1.141	3.90×10^{-4}	120↑
Metronidazole 6 weeks	-	-	-	-	-
Doxycycline 2 weeks	Induction	mmu-miR-6236	2.39	1.55×10^{-7}	126↓
		mmu-miR-5099	1.551	7.66×10^{-5}	1404↓
		mmu-miR-5121	1.337	5.85×10^{-5}	4001↓
		mmu-miR-1940	2.27	1.36×10^{-4}	*
		mmu-miR-1291	1.582	2.35×10^{-4}	4934↓
	Suppression	mmu-miR-409-5p	−1.778	4.35×10^{-6}	120↑
		mmu-miR-6240**	−2.231	1.43×10^{-4}	840↑
Doxycycline 6 weeks	Suppression	mmu-miR-144-3p	−1.338	1.64×10^{-4}	849↑
		mmu-miR-144-5p	−1.271	1.32×10^{-4}	2254↑
		mmu-miR-31-5p	−1.009	4.10×10^{-4}	414↑

Table 1. *Cont.*

B				
6 weeks vs. 2 weeks per Treatment	Regulation	microRNA	Log2FC	*p*-Value
Water	Suppression	mmu-miR-1940	−2.198	3.43×10^{-5}
		mmu-miR-877-3p	−1.648	3.43×10^{-5}
		mmu-miR-409-5p	−1.213	1.85×10^{-4}
		mmu-miR-485-3p	−1.472	1.60×10^{-4}
Seed oil	Suppression	mmu-miR-150-5p	−1.945	4.10×10^{-5}

* Sequence reported as miR-1940 appears to be a fragment of the snoRNA SCARNA4. The entry is removed from miRBase 21. ** mmu-miR-6240 is not confidently annotated but shares a seed with miR-330-3p.1 family and thus has the same predicted targets.

Regarding time-dependent changes in microRNA expression patterns, differential microRNA signatures were found when comparing the 6-week time point with the 2-week time point (Table 1B). During these 4 weeks, we found up to four microRNAs altered in the vehicle groups (water or seed oil (isotretinoin vehicle)), indicating the occurrence of relevant time-dependent microRNA-mediated effects over the selected time frame.

2.2. Integrative Pathway Analysis of Epigenetic Modifications in Iintestinal Epithelial Cells after Isotretinoin or Antibiotic Treatment

In Figure 3, a thorough pathway analysis based on the changes in the methylation status (Figure 3, left panel), and predicted microRNA targets by applying Metacore (Clarivate Analytics, Philadelphia, PA, USA) (Figure 3, right panel) is displayed. Both epigenetic modifications were correlated with the respective mRNA analysis (Figure 3, middle panel) to determine possible overlaps that might represent regulations on mRNA levels based on the changes at the epigenetic level.

2.2.1. DNA Methylation Pattern in Intestinal Epithelial Cells Directly after Isotretinoin or Antibiotic Treatment (Direct Effect)

Isotretinoin treatment resulted in the hypomethylation of 234 targets, and the subsequent induction of pathways involved in Granulocyte-Colony Stimulating Factor (G-CSF)-dependent stem cell mobilization ($p = 5.31 \times 10^{-4}$), regulation of epithelial-to-mesenchymal transition (EMT) ($p = 1.46 \times 10^{-3}$) and Slit-Robo signaling ($p = 1.54 \times 10^{-3}$), which plays an important role in developmental processes. When comparing the hypomethylated targets with the up-regulated mRNA data set, we identified one overlap interleukin (IL) 12rb1 (Figure 3A, left panel). The most significant pathways showing mRNA upregulation directly after isotretinoin treatment were associated with cell adhesion ($p = 7.29 \times 10^{-6}$), inhibitory PD-1 signaling ($p = 4.23 \times 10^{-6}$), and IL-12-induced interferon (IFN)-γ production ($p = 8.32 \times 10^{-5}$). The latter lead to the suggestion of a possible epigenetic mechanism in the regulation of the IFN-γ loci by IL-12 in isotretinoin-treated animals. Down-regulated mRNAs were involved in antiviral actions of interferons ($p = 3.64 \times 10^{-3}$), IL-33 signaling ($p = 4.72 \times 10^{-3}$), and tissue factor signaling in cancer ($p = 7.52 \times 10^{-3}$) (Figure 3A, middle panel). Since there were no hypermethylated targets, no overlaps were determined between the hypermethylated targets and down-regulated mRNAs.

Directly after metronidazole treatment, no altered pathways were identified due to the small number of hypo- (*Kcnt2*) or hypermethylated targets, indicating a minor effect of metronidazole on the DNA methylation status in IECs (Figure 3B, left panel).

Methylation patterns similar to metronidazole were also observed directly after doxycycline treatment, where small numbers of hypomethylated targets (*Vmn2r40*, *Esam*) or hypermethylated targets (*LOC100041346*) were identified (Figure 3C, left panel). These results point to a moderate effect of antibiotics on the DNA methylation status in IECs.
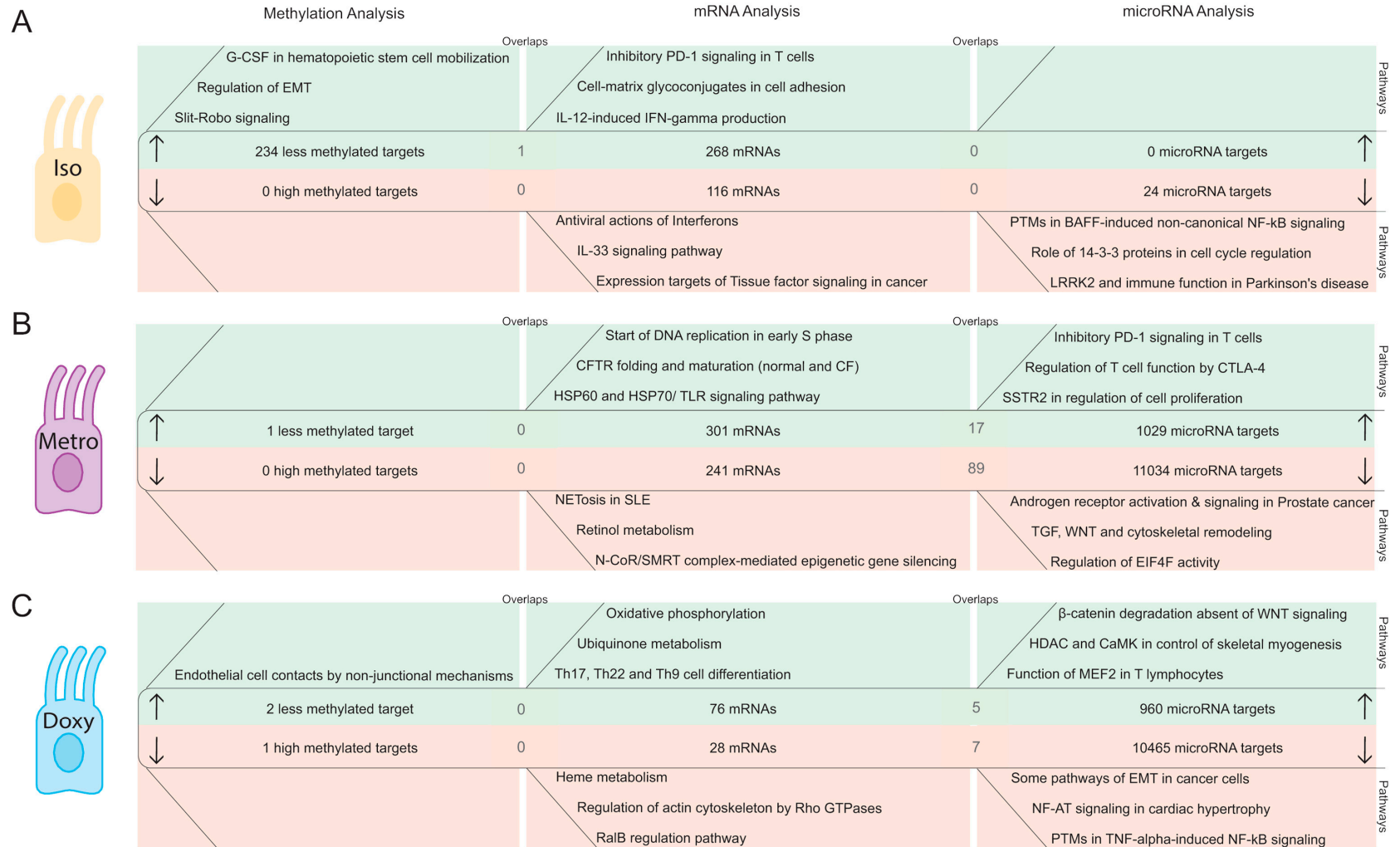
Figure 3. Integrative pathway studies of acute drug-induced epigenetic modifications in murine IECs. Analysis of differential DNA methylation and in silico predicted microRNA targets. For the latter, TargetScan or TargetScan custom were applied [29,30] in (**A**) isotretinoin (Iso), (**B**) metronidazole (Metro) and (**C**) doxycycline (Doxy) treated animals that were compared to the respective vehicles. Differentially expressed mRNAs were determined by applying: |log2 (fold change)| $\geq$ 0.5,

p-value ≤ 0.05 (middle panels). Three of the most significant pathways associated with hypomethylation (induced targets) and increased microRNA targets (decreased microRNAs), as well as mRNAs are shown in the green areas, whereas hypermethylation (suppressed targets) and decreased microRNA targets (increased microRNAs), as well as mRNAs are depicted in the red areas. Common candidates between in silico predicted microRNA targets and sequenced mRNAs (overlaps) are shown in the centers of the respective analysis. As for the pathway analysis, Metacore by Clarivate Analytics, Philadelphia, PA, USA was applied. G-CSF = Granulocyte-Colony Stimulating Factor; EMT = Epithelial Mesenchymal Transition; PD-1 = Programmed cell death protein 1; PTM = Post-transcriptional modification; BAFF = B-cell activating factor; NFkB = Nuclear factor kappa-light-chain-enhancer of activated B cells; LRRK2 = Leucine-rich repeat kinase 2; CFTR = Cystic Fibrosis Transmembrane Conductance Regulator; CF = Cystic Fibrosis; HSP60 = Heat shock protein 60; TLR = Toll-like receptor; NET = Neutrophil extracellular traps; SLE = Systemic lupus erythematosus; N-CoR = Nuclear receptor co-repressor; SMRT = Silencing mediator of retinoic acid and thyroid hormone receptor; SSTR2 = Somatostatin receptor 2; TGF = Transforming growth factor; EIF4F = Eukaryotic initiation factor 4F; GTP = Guanosine-5′-triphosphate; RalB = Ras-related protein Ral-B; HDAC = Histone deacetylases; CaMK = Ca2+/calmodulin-dependent protein kinase; MEF2 = Myocyte enhancer factor-2; NF-AT = Nuclear factor of activated T-cells; TNF = Tumor necrosis factor.

2.2.2. MicroRNA Expression Pattern in Intestinal Epithelial Cells Directly after Isotretinoin or Antibiotic Treatment (Direct Effect)

Comparing predicted microRNA targets with the corresponding mRNAs directly after isotretinoin treatment revealed only a moderate effect on microRNA-mediated silencing, with 24 potentially down-regulated microRNA targets (Figure 3A, right panel). These 24 down-regulated microRNA targets were involved in post-transcriptional modifications in B-cell activating factor (BAFF)-induced nuclear factor (NF)-κB signaling ($p = 6.54 \times 10^{-4}$), cell cycle regulation ($p = 2.49 \times 10^{-2}$), and LRRK2 processes ($p = 2.49 \times 10^{-2}$).

Metronidazole induced a different expression profile compared to isotretinoin, with 1029 potentially up-regulated microRNA targets from which 17 corresponded to the mRNA dataset and are presented as overlaps in Table S1B. The up-regulated 301 mRNAs in the presence of metronidazole were associated with cell cycle ($p = 2.30 \times 10^{-9}$), and microbial sensing processes ($p = 3.25 \times 10^{-4}$). Metronidazole significantly affected microRNA-mediated mRNA-silencing via the induction of five microRNAs, which potentially suppressed 11,034 microRNA targets. This led to 89 overlaps between down-regulated mRNAs and potentially suppressed microRNA targets that were involved in putative pathways of hormone action in neurofibromatosis type 1, NETosis in SLE, and extra-cellular matrix (ECM) remodeling in cell adhesion (Table S1B). In the mRNA analysis, 241 down-regulated mRNAs were associated with NETosis in SLE ($p = 2.39 \times 10^{-5}$), retinol metabolism ($p = 1.36 \times 10^{-3}$), and N-CoR/SMRT epigenetic silencing ($p = 2.31 \times 10^{-3}$) (Figure 3B, middle panel), indicating that mechanisms of NETosis might be of relevance in metronidazole treatment.

Doxycycline treatment suppressed two microRNAs directly after treatment cessation that resulted in 960 potentially induced microRNA targets as determined by TargetScan [29,30]. These 960 microRNA targets were involved in β-catenin degradation absent of Wingless-type MMTV integration site family (WNT) signaling ($p = 2.00 \times 10^{-7}$), histone deacetylase (HDAC), and calcium/calmodulin-dependent kinase (CaMK), which controls skeletal myogenesis ($p = 4.59 \times 10^{-7}$), and the function of MEF2 in T lymphocytes ($p = 2.33 \times 10^{-6}$). Interestingly, five overlaps were identified when comparing the induced mRNA and microRNA target datasets that were associated with immunomodulatory processes, for instance, IL-17 signaling pathway ($p = 7.27 \times 10^{-3}$) (Table S1B). Accordingly, we observed a trend towards a pro-inflammatory profile directly after doxycycline treatment, where 76 mRNAs were involved in Th17, Th22, and Th9 cell differentiation ($p = 5.91 \times 10^{-4}$), ubiquinone metabolism ($p = 1.42 \times 10^{-5}$), and oxidative phosphorylation ($p = 4.08 \times 10^{-10}$) (Figure 3C, middle panel). Doxycycline induced five microRNAs that potentially decreased 10,465 microRNA targets, which were associated with EMT in cancer cells ($p = 1.35 \times 10^{-9}$), Nuclear factor of activated T-cells (NF-AT) signaling in cardiac hypertrophy ($p = 2.22 \times 10^{-8}$), and post-transcriptional phosphorylation in tumor necrosis factor-induced NF-κB signaling ($p = 2.48 \times 10^{-8}$). With the experimentally derived 28 down-regulated mRNAs, we identified seven overlaps, which were involved in diverse transport processes (Table S1B).

2.2.3. DNA Methylation Pattern in Intestinal Epithelial Cells after the Washout Phase of Isotretinoin or Antibiotic Treated Groups (Long-Term Effects)

Four weeks after the last isotretinoin application, moderate effects were observed in isotretinoin-treated animals compared to the vehicle group (Figure 4A, left panel). Only eight hypermethylated targets involved in sphingolipid metabolism ($p = 9.90 \times 10^{-3}$) were found, with no overlaps with the mRNA dataset. These results indicate a reversible effect since we observed strong demethylation properties directly after isotretinoin treatment, which were not present after the washout phase. Previous treatment with metronidazole resulted in only one hypomethylated target compared to the vehicle group (i.e., *Lmx1a*), indicating an overall negligible direct and long-term impact on DNA methylation (Figure 4B, left panel).
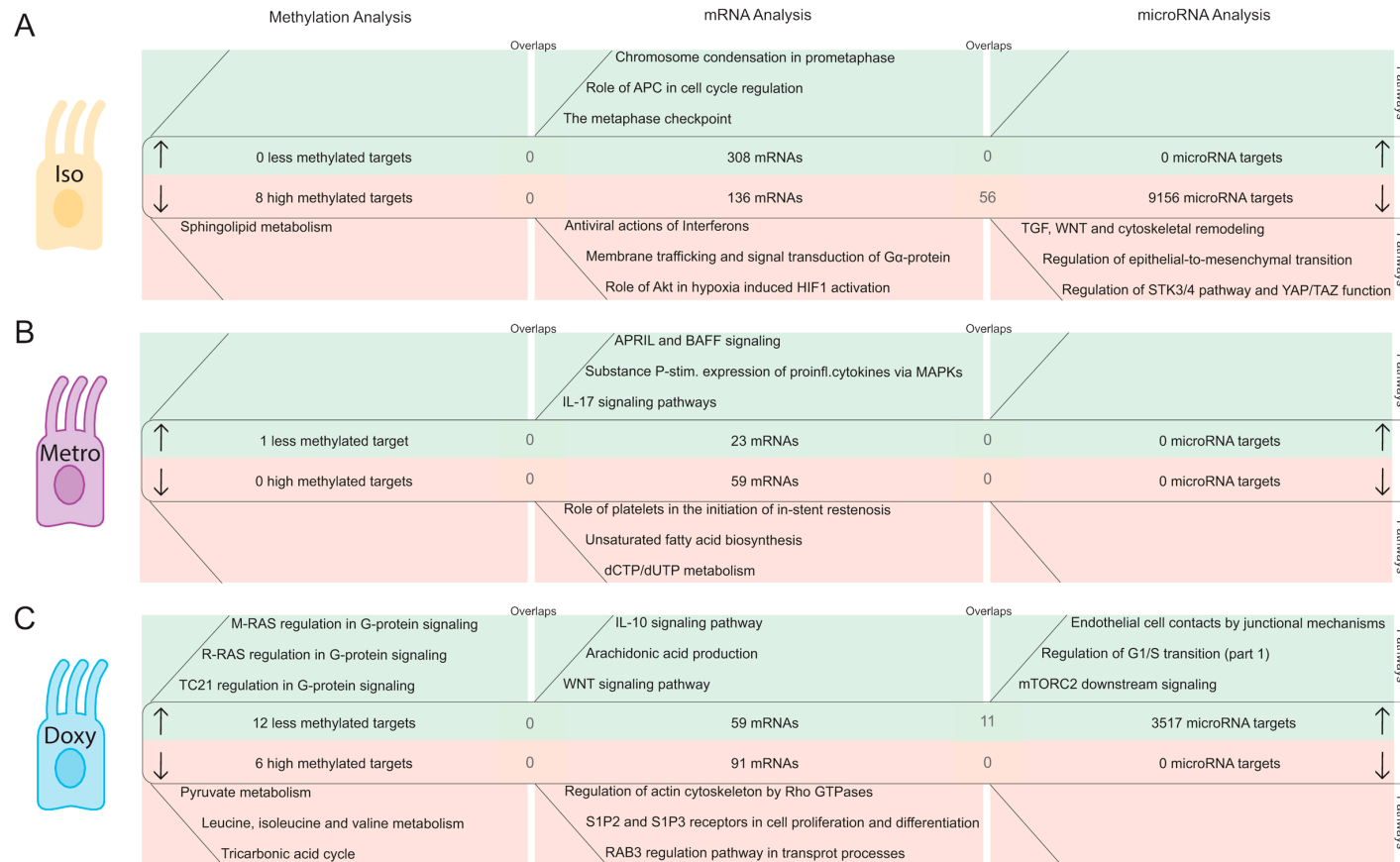
Figure 4. Integrative pathway studies of long-term drug-induced epigenetic modifications in murine IECs. Analysis of differential DNA methylation and in silico predicted microRNA targets. For the latter, TargetScan or TargetScan custom [29,30] were applied in (**A**) isotretinoin (Iso), (**B**) metronidazole (Metro) and (C) doxycycline (Doxy) treated animals that were compared to respective vehicles. Differentially expressed mRNAs were determined by applying: |log2 (fold change)| ≥ 0.5, *p*-value ≤ 0.05 (middle panels). Three of the most significant pathways associated with hypomethylation (induced targets) and increased microRNA targets (decreased microRNAs), as well as mRNAs are shown in the green areas, whereas hypermethylation (suppressed targets) and decreased microRNA targets (increased microRNAs), as well as mRNAs are depicted in the red areas. Common candidates between in silico predicted microRNA targets and sequenced mRNAs (overlaps) are shown in

the centers of the respective analysis. As for the pathway analysis, Metacore by Clarivate Analytics, Philadelphia, PA, USA was applied. APC = Antigen presenting cell; Akt = Protein kinase B/ AKT8 virus oncogene cellular homolog; HIF1 = Hypoxia-inducible factor 1; STK3/4 = Serine/Threonine-Protein Kinase 3; YAP = Yes-associated protein; TAZ = Transcriptional co-activator with PDZ-binding motif; APRIL = A proliferation-inducing ligand; MAPK = Mitogen-activated protein kinase; dCTP = Deoxycytidine triphosphate; dUTP = Deoxyuridine triphosphate; mRAS = muscle RAS oncogene homolog; rRAS = Ras-related protein; TC21 = Related RAS viral (r-ras) oncogene homolog 2/ RRAS2; S1P = Sphingosine-1-phosphate; RAB3 = Ras-related in brain/ GDP/GTP exchange protein 3; mTORC = Mammalian target of rapamycin complex 2.

After the washout phase, 12 hypomethylated targets were associated with G-protein signaling ($p = 9.95 \times 10^{-3}$), and six hypermethylated targets were determined in doxycycline-treated animals. These six suppressed targets were involved in pyruvate metabolism ($p = 4.64 \times 10^{-5}$), amino acid metabolism ($p = 8.92 \times 10^{-3}$), and the tricarbonic acid cycle ($p = 1.16 \times 10^{-2}$) (Figure 4C, left panel). These small numbers were not sufficient to determine overlaps between the differentially methylated targets and mRNA datasets.

2.2.4. MicroRNA Expression Pattern in Intestinal Epithelial Cells after the Washout Phase of Isotretinoin or Antibiotic Treated Groups (Long-Term Effect)

Isotretinoin induced the expression of two microRNAs (microRNA-98-3p, -142b) after the washout phase that potentially suppress 9156 microRNA targets. Significant results after analysis with Metacore by Clarivate Analytics pointed to signaling pathways associated with Transforming growth factor (TGF), WNT, and cytoskeleton remodeling ($p = 1.32 \times 10^{-12}$), regulation of EMT ($p = 4.63 \times 10^{-10}$), and negative regulation of the Serine/Threonine-Protein Kinase (STK) 3/4 pathway and positive regulation of Yes-associated protein (YAP)/ Transcriptional co-activator with PDZ-binding motif (TAZ) function ($p = 6.42 \times 10^{-10}$). We determined 56 mRNAs as overlaps between the microRNA targets and mRNA datasets, which were involved in IL-6 signaling ($p = 6.99 \times 10^{-3}$). The corresponding down-regulated 136 mRNAs were associated with antiviral infection pathways ($p = 2.17 \times 10^{-3}$), membrane trafficking and signal transduction of Gα protein ($p = 3.95 \times 10^{-3}$), as well as protein kinase B (Akt) in hypoxia ($p = 7.91 \times 10^{-3}$). No down-regulated microRNAs were determined upon isotretinoin treatment after the washout phase, and henceforth no microRNA targets were predicted by TargetScan [29,30]. However, 308 up-regulated mRNAs were associated with diverse cell cycle processes ($p = 1.11 \times 10^{-15}$) (Figure 4A, middle panel).

Metronidazole had no impact on microRNA expression after the washout phase. Yet, metronidazole up-regulated 23 mRNAs involved in a proliferation-inducing ligand (APRIL) and BAFF signaling ($p = 7.06 \times 10^{-4}$), the expression of pro-inflammatory cytokines via Mitogen-activated protein kinases (MAPKs) ($p = 8.59 \times 10^{-4}$), and IL-17 signaling ($p = 1.67 \times 10^{-3}$). Furthermore, 59 down-regulated mRNAs were associated with the initiation of restenosis ($p = 5.06 \times 10^{-3}$), fatty acid biosynthesis ($p = 1.03 \times 10^{-2}$), and dCTP/dUTP metabolism ($p = 1.48 \times 10^{-2}$).

Doxycycline down-regulated three microRNAs (microRNA-144-3p, -144-5p, -31-5p) after the washout phase. These three microRNAs resulted in the prediction of 3517 microRNA targets involved in endothelial cell contacts by junctional mechanisms ($p = 9.64 \times 10^{-7}$), regulation of G1/S transition ($p = 1.02 \times 10^{-6}$), and mammalian target of rapamycin complex 2 (mTORC2) downstream signaling ($p = 2.20 \times 10^{-6}$). Within this dataset, we identified 11 overlaps with the mRNA dataset. The pathways determined using Metacore by Clarivate Analytics for the 11 overlaps were involved in immune responses ($p = 1.86 \times 10^{-2}$), apoptosis and survival ($p = 2.32 \times 10^{-2}$), as well as colorectal cancer ($p = 2.77 \times 10^{-2}$) (Table S1B). The 59 significantly induced mRNAs were associated with IL-10 signaling ($p = 5.57 \times 10^{-5}$), arachidonic acid production ($p = 6.09 \times 10^{-4}$), and WNT signaling ($p = 7.67 \times 10^{-4}$). Previous treatment with doxycycline did not lead to a down-regulation of microRNA targets, yet, 91 down-regulated mRNAs (Figure 4C, middle panel) were involved in Rho GTPases-dependent cytoskeleton regulation ($p = 1.39 \times 10^{-4}$), S1P2 and S1P3-mediated cell proliferation and differentiation ($p = 2.02 \times 10^{-4}$), as well as Ras-related protein Rab-3(RAB3) regulation in transport processes ($p = 1.72 \times 10^{-3}$). We did not identify any overlaps in the down-regulated datasets.

2.3. Time-Dependent Changes in Epigenetic Mechanisms in Murine Colonic Intestinal Epithelial Cells

We further studied time-dependent effects in murine IECs by comparing the 6-week with the 2-week time points of the vehicle groups to elucidate epigenetic changes occurring over a 4-week time frame (average life span of a mouse is 2 years). Figure 5 depicts a pathway analysis based on changes in the DNA methylation pattern and the expression of microRNA targets that were compared to differentially expressed mRNAs for water and seed oil-treated groups.
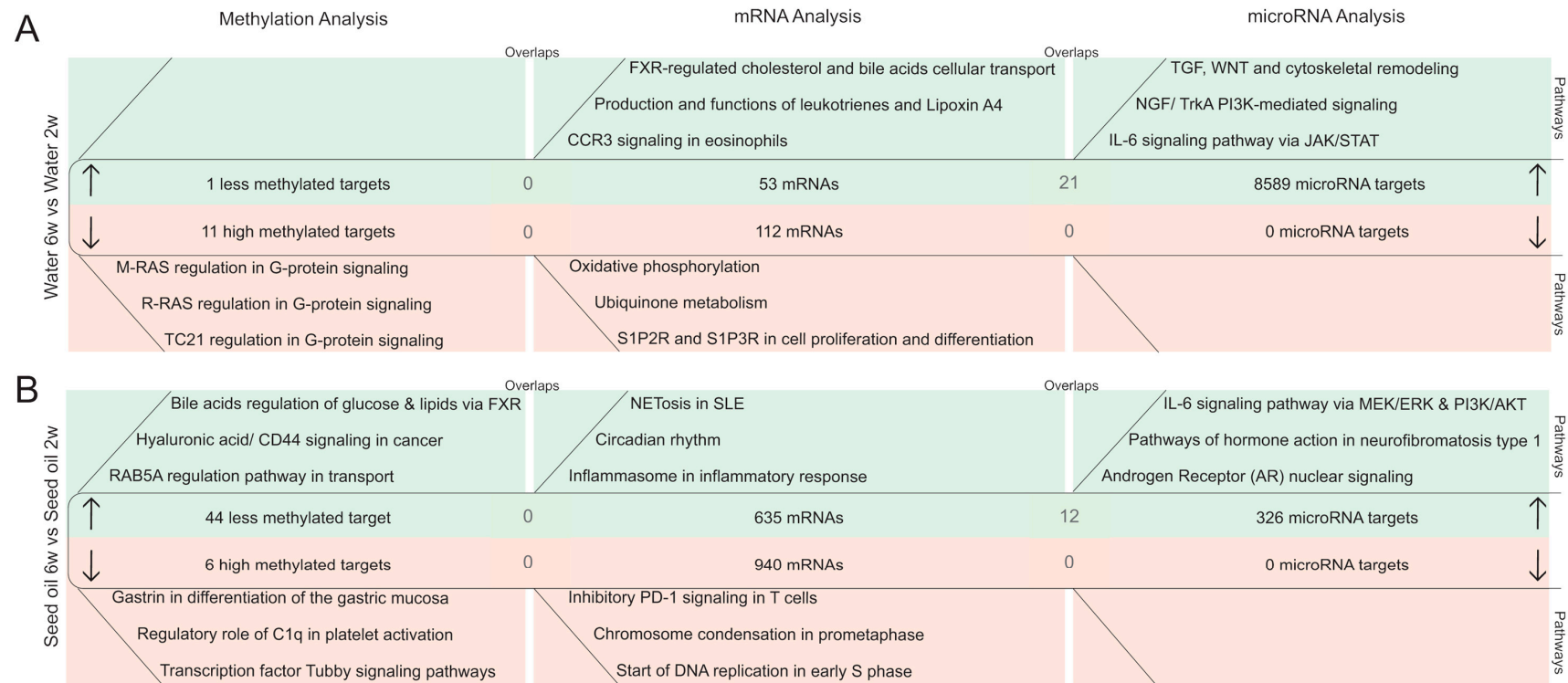
Figure 5. Integrative studies of time-dependent epigenetic modifications in murine IECs. For identifying alterations that might occur over time, the 6-week time point was compared to the 2-week time point (reference group). Differential DNA methylation (left) and mathematically predicted microRNA targets (right) were analyzed by applying Metacore by Clarivate Analytics and TargetScan or TargetScan custom [29,30]. Differentially expressed mRNAs were selected with: |log2 (fold change)| ≥ 0.5, *p*-value ≤ 0.05 (middle panels). Three of the most significant pathways associated with hypomethylation (induced targets) and increased microRNA targets (decreased microRNAs), as well as mRNAs are shown in the green areas, whereas hypermethylation (suppressed targets) and decreased microRNA targets (increased microRNAs), as well as mRNAs are depicted in the red areas. Common candidates between in silico predicted microRNA targets and sequenced mRNAs (overlaps) are shown in the centers of the respective analysis. (**A**) Changes at the basal level of water-treated animals, (**B**) seed oil treated animals that were compared to the respective 2-week reference group. TC21 = Related RAS viral (r-ras) oncogene homolog 2/ RRAS2; FXR = Farnesoid X receptor; NGF = Nerve growth factor; TrkA = Tropomyosin-related kinase; PI3K = Phosphatidylinositiol-3-Kinase; RAB5A = Ras-related in brain/ GDP/GTP exchange protein 5A; C1q = First complement subcomponent; MEK = MAPK/Erk kinase; ERK = Extracellular signal-regulated kinase.

In water-treated animals, we determined 11 hypermethylated targets that were associated with diverse G-protein signaling pathways ($p = 9.95 \times 10^{-3}$) without any overlaps with the mRNA dataset (Figure 5A, left panel). Time-dependent changes in DNA methylation in animals treated with seed oil (Figure 5B) were comparable to the water-treated group. In total, 44 hypomethylated targets were associated with bile acids regulation of glucose and lipid metabolism via farnesoid X receptor (FXR) ($p = 7.06 \times 10^{-4}$), CD44 signaling in cancer ($p = 1.56 \times 10^{-3}$), and the GDP/GTP exchange protein (RAB) 5A regulation pathway ($p = 2.57 \times 10^{-2}$). Six suppressed targets through hypermethylation were associated with gastrin-dependent differentiation of the gastric mucosa ($p = 1.51 \times 10^{-4}$), platelet activation by the complement subcomponent C1q ($p = 7.77 \times 10^{-3}$), and transcription factor Tubby signaling pathways ($p = 8.81 \times 10^{-3}$).

In contrast with the moderate time-dependent effects on DNA methylation at the basal level, the analysis of differentially expressed microRNAs and their potential targets revealed strong microRNA-mediated alterations, in both vehicle groups with possible epigenetic regulation at the mRNA level. Time-dependent effects in water-treated animals led to the suppression of four microRNAs and the prediction of 8589 microRNA targets by TargetScan [29,30]. These potentially induced targets were associated with TGF, WNT, and cytoskeletal remodeling ($p = 4.32 \times 10^{-16}$), nerve growth factor (NGF)/TrkA PI3K-mediated signaling in apoptosis and survival ($p = 1.04 \times 10^{-12}$), and IL-6 signaling pathway via JAK/STAT ($p = 3.00 \times 10^{-11}$). This dataset enabled the determination of 21 overlaps with the mRNA dataset (Figure 5A, right panel) associated with cellular transport and metabolism processes (Table S1C). The 53 induced mRNAs were involved in FXR-regulated cholesterol, and bile acid cellular transport ($p = 4.38 \times 10^{-6}$), production and main functions of biologically active leukotrienes, and Lipoxin A4 ($p = 7.95 \times 10^{-3}$), and immunologically relevant C-C chemokine receptor type 3 (CCR3) signaling in eosinophils ($p = 1.82 \times 10^{-2}$). No down-regulated microRNA targets were identified in the water-treated groups over time. Yet, 112 down-regulated mRNAs were involved in oxidative phosphorylation ($p = 4.49 \times 10^{-8}$), ubiquinone metabolism ($p = 7.97 \times 10^{-7}$), and S1P2 and S1P3 receptors in cell proliferation and differentiation ($p = 3.04 \times 10^{-5}$).

Time-dependent changes in the seed oil vehicle group were less pronounced; only microRNA-150-5p was suppressed. Suppression of microRNA-150-5p potentially induced 326 microRNA targets that were associated with the IL-6 signaling pathway via MEK/ERK and PI3K/AKT signaling cascades ($p = 1.66 \times 10^{-5}$), pathways of hormone action in neurofibromatosis type 1 ($p = 3.34 \times 10^{-5}$), and androgen receptor nuclear signaling in transcription ($p = 5.96 \times 10^{-5}$). The identification of 12 overlaps between the microRNA target and mRNA dataset indicate possible epigenetic regulation through microRNAs (Table S1C). The analysis of up-regulated mRNAs in seed oil treated groups revealed pathways involved in NETosis in SLE ($p = 5.84 \times 10^{-7}$), circadian rhythm ($p = 1.66 \times 10^{-5}$), and inflammasome involvement in inflammatory response ($p = 1.35 \times 10^{-3}$). By applying our strict thresholds, we were not able to identify up-regulated microRNAs, and therefore no overlaps were found. However, we identified 940 time-dependent suppressed mRNAs, which were associated with inhibitory PD-1 signaling in T cells ($p = 5.26 \times 10^{-11}$), and cell cycle processes ($p = 2.68 \times 10^{-10}$) (Figure 5B, middle panel).

3. Discussion

Epigenetic modifications are well known to play an important role in many fundamental biological processes, such as cell-specific differentiation, development and function [31,32]. Mounting evidence suggests that epigenetic mechanisms are altered in several diseases, including IBD [33]. In the present study, we aimed to identify differential drug- and time-dependent epigenetic modifications in murine IECs to gain a better understanding of the influence of medication on the risk of developing IBD.

Despite the increasing body of literature correlating DNA methylation with development and inheritable susceptibility of intestinal inflammation [34,35], an association between epigenetically modified genes does not immediately prove a relation to their functionality. Verification of a causative relationship between an epigenetic mark and gene expression remains one of the major challenges

because these marks undergo dynamic changes during cell development, cellular homeostasis and stress, as well as disease onset [36]. An important advantage of this study is the robust approach to analyze methylome-wide alterations through the methyl-binding domain (MBD) enrichment strategy [37,38]. Additionally, correlation of the DNA methylation status with the corresponding transcriptome in colonic IECs per mouse without any pooling represents an additional advantage compared to whole tissue samples and restricted microarray panels. Furthermore, this study also includes microRNA-mediated modifications leading to a thorough epigenetic overview of direct and long-term drug-induced, as well as time-dependent effects. It also has to be added that whole-methylome studies and parallel analysis of microRNA and mRNA expression in IECs using next generation sequencing are sparse. Furthermore, analysis of microRNA expression and its impact on cellular processes remains challenging due to difficulties in normalization and the complex microRNA–mRNA interactions, as incomplete sequence alignment is often sufficient to suppress microRNA targets [39].

For reliable identification of methylated targets and regulated microRNAs, we used stringent thresholds in our computational processing ($|\log2 \text{ (fold change)}| \geq 1$, p-value ≤ 0.001). However, harsh thresholds for determination of altered methylation and microRNA expression might preclude identification of further hits of relevance.

Treatment with the vitamin A derivate isotretinoin led to the demethylation of targets that were involved in IL-12 signaling and developmental processes, including the hypomethylated target IL-12rb1 and the corresponding up-regulated IL-12-dependent pathway in the transcriptome analysis directly after isotretinoin treatment in IECs. Our previous studies showed a systemic decrease in serum IL-12p40 levels [20], and no impact on the course of colitis after isotretinoin treatment in DSS- and T-cell-transfer colitis models. Furthermore, isotretinoin induced an anti-inflammatory immune cell profile in vitro and in vivo [21,28]. Pedrotti et al. described local intestinal effects on lamina propria cells after systemic changes of IL-12 levels [40]. Thus, it is tempting to speculate that the previously described decrease of systemic IL-12p40 levels is affecting local IECs by up-regulating IL-12rb1 through a negative feedback mechanism that has been described for IL-7/IL-7R on T-cells [41,42]. The effects of an increased expression of IL-12rb1 in IECs have not yet been studied. However, Lin and colleagues have identified the aberrant methylation pattern of the gene encoding IL-12b in peripheral B cells of IBD patients [43]. Moreover, genome-wide association studies have shown that IL-12-/IL-23 signaling pathways contain crucial susceptibility gene loci in IBD [44]. Thus, further studies are needed to elucidate whether the increased expression of IL-12rb1 might be associated with adverse effects in the intestine. Although epigenetic marks such as DNA methylation are long-lasting and inheritable modifications, isotretinoin-induced demethylation was resolved after the washout phase of 4 weeks, indicating short-term effects on IL-12rb1. Furthermore, isotretinoin did not affect IBD-associated microRNAs in IECs neither directly after treatment cessation nor after the washout phase.

It is generally observed that intestinal inflammation is dependent on lymphocyte trafficking to mucosal tissue via adhesion markers, such as alpha4beta7 integrin and mucosal vascular addressing cell adhesion molecule 1 (Madcam1), enabling the intestinal entrance of CD4+ and CD8+ T cells and thereby supporting the pro-inflammatory response of IBD patients. Blocking the interaction between alpha4beta7 and Madcam1 attenuates inflammation in IBD patients [45,46]. In our previous transcriptome study in T cells, we did not observe an increase of those gut-homing markers in CD4+ CD25+ and CD4+ CD62L+ T cells on mRNA level directly after isotretinoin treatment and later on [28]. Interestingly, when analyzing the transcriptome of IECs after isotretinoin treatment, we also did not identify an increase of the aforementioned adhesion markers but an upregulation of tolerance-associated surface integrins, such as ITGAE (CD103) and ITGAX (CD11c) [47,48] on mRNA level in IECs. These results indicate that isotretinoin is not associated with an altered expression of adhesion molecules that might lead to an exaggeration of an inflammatory condition in the gut.

In contrast to isotretinoin, doxycycline and metronidazole had only a moderate impact on the DNA methylation status, while both antibiotics induced pronounced short-term microRNA-mediated

changes, which in the case of metronidazole mostly resolved. In this large-scale study, we also identified doxycycline-induced mRNAs associated with oxidative metabolism and pro-inflammatory responses directly after treatment. However, anti-inflammatory properties of tetracyclines have been described. D'Agostino et al. reported a suppression of nitric oxide synthase by tetracycline in macrophages, thereby inhibiting the generation of oxygen radicals [49]. Furthermore, tetracyclines have been shown to have beneficial immunomodulatory properties in several inflammatory conditions, such as multiples sclerosis, Parkinson's disease and rheumatoid arthritis [50]. However, recent epidemiological reports have identified doxycycline to be associated with CD (OD 2.25), pointing to adverse effects in the gut [22]. In the present study, we observed an elevation of the pro-inflammatory IL-17 signaling pathway as found in the transcriptome analysis and in the overlaps with the microRNA target dataset in IECs of doxycycline-treated animals. However, the latter findings require further investigations. It would be interesting to analyze the mRNA and microRNA expression patterns in appropriate animal models or human biopsies to better translate the mechanisms of the acute effects after doxycycline treatment from mice into humans since many immune pathways and epigenetic mechanisms are conserved among mammals.

Interestingly, we observed persistent microRNA-mediated modifications after the washout phase upon treatment with doxycycline. The majority of studies have investigated solely the immediate impact after doxycycline treatment, therefore and to the best of our knowledge, this study is showing, for the first time, long-term effects of orally applied doxycycline on IECs. Interestingly, long-term effects of doxycycline showed an anti-inflammatory signature in IECs mediated by the up-regulation of IL-10 signaling, which contrasted with the direct effects of doxycycline. These results suggest not only reversible effects of doxycycline, but indicate potential tolerance-inducing properties in the murine colon. Whether these effects of oral doxycycline treatment are mediated directly or indirectly by modulating the gut microbiota through the reduction of *Lachnospiraceae* [51] needs further investigations. In this context, Nakanishi et al. [52] reported that vancomycin-mediated reduction of *Lachnospiraceae* ameliorated colitis by selectively blocking the recruitment of infiltrating inflammatory monocytes/macrophages, supporting possible indirect mechanisms upon the treatment with doxycycline. Since the composition of the commensal gut microbiota is similar between humans and rodents, further studies need to be performed in human stool samples and PBMCs after doxycycline treatment that provide a better understanding of the direct and long-term effects in humans.

Additional analysis of time-dependent alterations in murine IECs showed moderate DNA methylation changes at the basal level, pointing to stable epigenetic marks over the selected time frame of 4 weeks. The characterization of time-dependent microRNA modifications in IECs revealed four microRNAs (mmu-miR-1940, -877-3p, -409-5p, -485-3p) that were down-regulated over time and might represent time-sensitive epigenetic modifications. These microRNAs are described for the first time in this study and require further investigations to elucidate how these four microRNAs are involved in maturation and developmental processes in IECs.

Our study reports, for the first time, profound comparisons between DNA methylation and differential microRNA expression with the respective mRNA expression, which might represent the basis for further investigations and possibly help to unravel environmental mechanisms affecting gut homeostasis that can be further applied into human settings.

In summary, integrative large-scale epigenetic analysis upon isotretinoin and doxycycline treatment revealed an induction of a pro-inflammatory immune profile directly after treatment cessation, in contrast to metronidazole, which promoted a trend towards anti-inflammatory signaling at the microRNA level. After the washout phase, the pro-inflammatory effects of isotretinoin and doxycycline resolved, and were accompanied by beneficial immunomodulatory processes. Metronidazole treatment induced no long-term effects on epigenetic level in IECs. Furthermore, both antibiotics had only a moderate impact on DNA methylation, in contrast to isotretinoin, which exhibited acute demethylation properties affecting IL-12 signaling and developmental processes.

Importantly, these demethylating effects resolved after the washout phase and do not support long-term epigenetic modifications after isotretinoin treatment that might influence an association with a development of IBD later on.

4. Materials and Methods

4.1. Animals

Female Balb/c mice were purchased from Charles River Laboratories (Germany, Sulzfeld) and kept in the animal facility of the University Hospital Zurich under specific pathogen-free conditions and with ad libitum access to food and water.

4.2. Ethics Approval

All animal experiments were approved by the cantonal veterinary office of Zurich under licenses ZH-54-2011 and ZH-214-2016 and the methods were performed in accordance with the institutional and state guidelines.

4.3. Study Design

Animals were randomized according to body weight prior to treatment beginning and animals of the individual treatment groups were housed separately. The age of the mice was approximately 6 weeks when treatment was initialized. IECs were collected from each mouse straight after the 2-weeks treatment (immediate effects; age of mice was 8 weeks), and after a washout period of 4 weeks (week 6) without any treatment (long-term effects; age of mice was 12 weeks) (Figure 1). Female animals were used to allow comparability to our previous colitis studies where we used the same strain and sex. Furthermore, it is known that the incidence of autoimmune disease is higher in females than in males, at least in humans. Hence, we focused on female mice to better understand the potential adverse effects on this population.

The mice were treated daily for 2 weeks by oral gavage with therapeutically applied human doses that were normalized to mice: isotretinoin 30 mg/mL (human dose: 2 mg/kg) (F. Hoffmann-La Roche Ltd., Basel, Switzerland), or seed oil (*Brassica rapa*), metronidazole 107 mg/kg (human dose: 7.14 mg/kg) or doxycycline 43 mg/kg (human dose: 2.86 mg/kg) (Sigma-Aldrich, Buchs, Switzerland) or water. In the experiments with isotretinoin and antibiotics for DNA methylation, microRNA expression and mRNA analysis, 6 mice were analyzed individually per time point and treatment (*n* = 6 animals/time point/treatment). 5-aza-2′-deoxycytidine (DAC) was diluted in water and administered intraperitoneal 4 times with 3–4 days break between the 4 drug administrations. An amount of 1 mg/kg DAC was applied and adjusted to the body weight of each mouse. Four animals in the DAC or water-treated group were analyzed individually at the 2-week time point only to rank the DNA methylation-modifying properties of the aforementioned drugs. DAC served as a positive control from which it is known to significantly alter the DNA methylation pattern.

4.4. Isolation of Murine Intestinal Epithelial Cells from the Colon

A standard protocol was used for isolating IECs. Briefly, the colon was cut lengthwise, freed from residual faeces and cut into small pieces. To loosen IECs, the pieces were transferred to ice cold Hank's balanced salt solution (HBSS; PAA, Pasching, Austria) supplemented with 2 mM ethylenediaminetetraacetic acid (EDTA) and incubated for 30 min at 37 °C with continuous stirring. Mucosal tissue was collected by passing the slurry through a cell strainer (70 μm; Falcon, Corning, New York, NY, USA). The tissue residue was resuspended in fresh ice cold HBSS, vigorously shaken 10 times and vortexed for 1 min. Shaking and vortexing were repeated 2 more times resulting in 30 times shaking and 3 min of vortexing. Mucosal debris was separated from detached cells by filtration through a cell strainer. The flow through of single epithelial cells was collected and centrifuged for 7 min at 400 g and 4 °C. The supernatant was discarded and the cell pellet washed with ice cold

phosphate-buffered saline (PBS) followed by centrifugation. The supernatant was removed carefully and the cell pellet resuspended in RLT Buffer from the DNA/RNA Mini Kit (Qiagen, Hilden, Germany), snap frozen in liquid nitrogen and stored at −80 °C. Because the efficiency of this method has been established previously in our laboratory, we used IECs immediately without additional evaluation.

4.5. Genomic DNA and Total RNA Procedures

After isolation of IECs as described above, extraction of genomic DNA and total RNA including small RNA was performed with the DNA/RNA Qiagen Mini Kit (Qiagen) according to the manufacturer's instructions. Genomic DNA and total RNA quality and quantity were analyzed on the TapeStation2200 (Agilent, Waldbronn, Germany). Genomic DNA was further processed with the MethylMiner Kit (Thermo Fisher, Reinach, Switzerland). In brief, genomic DNA was fragmented by sonification into 255 bp fragments (Covaris, Woburn, MA, USA). Methylated fragments were captured with methyl-binding domain beads and precipitated with NaCl in a step-wise approach according to the manufacturer's instructions. Before sequencing, methylated DNA fragments and total RNA (including small RNA fractions) were analyzed on the TapeStation2200 (Agilent).

4.6. Sequencing Procedures

4.6.1. Library Preparations

The mRNA libraries were prepared as previously described [28]. Briefly, the TruSeq Stranded mRNA Sample Prep Kit (Illumina Inc., San Diego, CA, USA) was used. Total RNA samples were reverse-transcribed into double-stranded cDNA. Fragments containing TruSeq adapters on both ends were selectively enriched with polymerase chain reaction (PCR). The product was a smear with an average fragment size of approximately 360 bp.

For the microRNA libraries, the NEB Next Multiplex Small RNA Sample Prep Kit (New England Biolabs Inc., Ipswich, MA, SA) was used. A detailed description was previously described [28].

Library preparation for methylated fragmented DNA (MBD-Seq) was performed with the NEB Next Ultra DNA Library Prep for Illumina (New England Biolabs, Ipswich, MA, USA). In brief, DNA samples (100 ng) were end-repaired, adapters were ligated to the fragmented DNA samples and fragments containing adapters on both ends were selectively enriched with PCR. Multiplex indices were also added during the PCR step.

The quality and quantity of all enriched libraries were validated using Qubit®(1.0) Fluorometer and the Tapestation. All libraries were normalized to 10 nM in Tris-Cl 10 mM, pH 8.5 with 0.1% Tween 20.

4.6.2. Clustering and Sequencing

The TruSeq SR Cluster Kit v4-cBot-HS or TruSeq PE Cluster Kit v4-cBot-HS (Illumina Inc.) was used for cluster generation working with 8 pM for mRNA, 10 nM for smallRNA and 5 pM for DNA of pooled normalized libraries on the cBOT. Sequencing was performed on the Illumina HiSeq 2000 single read at 1×125 bp for mRNA, single read at 1×50 bp for smallRNA and single read at 1×125 bp for DNA using the TruSeq SBS Kit v4-HS (Illumina Inc.). Reads were quality-checked with fastqc which calculates various quality metrics for the raw reads.

4.7. Bioinformatics

A detailed description of all steps can be found in [28]. Briefly, raw fastqc reads were first cleaned by removing adapter sequences. As for mRNA sequencing, we applied the count-based negative binomial model implemented in the software package edgeR (R version: 3.2.0, edgeR version: 3.10.2) to detect differentially expressed genes [53]. Genes showing altered expression with adjusted *p*-value ≤ 0.05 were considered differentially expressed (Benjamini and Hochberg method). Further selection of mRNAs was done with the following threshold: $|\log2 \text{ (fold change)}| \geq 0.5$,

p-value ≤ 0.001. As for microRNA sequencing, ncPRO (version 1.5.1) [54] was applied. Differentially expressed microRNAs were identified applying edgeR and further selection of microRNAs was done with the following thresholds: |log2 (fold change)| ≥ 1, *p*-value ≤ 0.001. MicroRNA–mRNA correlation analysis was done with TargetScan (mouse, Version 7.1) and TargetScan custom (mouse, Version 5.2) [29,30]. Determination of pathways was performed with Metacore by Clarivate Analytics (Version 6.28). For identification of significant pathways within Metacore, Fisher's exact test and correction for multiple samples testing by FDR was applied.

DNA Methylation-Sequencing

The alignment of preprocessed reads was performed with Bowtie2 (version 2.2.1) [55] using the extra-option 'non-deterministic'. Quantification of CpG-island-sites was done using the count overlaps-method of the R-package Genomic Ranges. CpG islands in the mouse genome (build GRCm38) were predicted using the R-package make CGI (version 1.1) [56]. The statistical analysis of the resulting count data was performed using edgeR.

4.8. Statistics

Statistical analysis was performed by two-tailed Student's *t*-test. *p*-values ≤ 0.05 were considered statistically significant.

References

1. Molodecky, N.A.; Soon, I.S.; Rabi, D.M.; Ghali, W.A.; Ferris, M.; Chernoff, G.; Benchimol, E.I.; Panaccione, R.; Ghosh, S.; Barkema, H.W.; et al. Increasing incidence and prevalence of the inflammatory bowel diseases with time, based on systematic review. *Gastroenterology* **2012**, *142*, 46–54. [CrossRef] [PubMed]

2. Khor, B.; Gardet, A.; Xavier, R.J. Genetics and pathogenesis of inflammatory bowel disease. *Nature* **2011**, *474*, 307–317. [CrossRef] [PubMed]

3. Iborra, M.; Bernuzzi, F.; Invernizzi, P.; Danese, S. MicroRNAs in autoimmunity and inflammatory bowel disease: Crucial regulators in immune response. *Autoimmun. Rev.* **2012**, *11*, 305–314. [CrossRef] [PubMed]

4. Pekow, J.R.; Kwon, J.H. MicroRNAs in inflammatory bowel disease. *Inflamm. Bowel Dis.* **2012**, *18*, 187–193. [CrossRef] [PubMed]

5. Kalla, R.; Ventham, N.T.; Kennedy, N.A.; Quintana, J.F.; Nimmo, E.R.; Buck, A.H.; Satsangi, J. MicroRNAs: New players in IBD. *Gut* **2015**, *64*, 504–517. [CrossRef] [PubMed]

6. Ma, X.; Zhou, J.; Zhong, Y.; Jiang, L.; Mu, P.; Li, Y.; Singh, N.; Nagarkatti, M.; Nagarkatti, P. Expression, regulation and function of microRNAs in multiple sclerosis. *Int. J. Med. Sci.* **2014**, *11*, 810–818. [CrossRef] [PubMed]

7. Huang, R.Y.; Li, L.; Wang, M.J.; Chen, X.M.; Huang, Q.C.; Lu, C.J. An Exploration of the Role of MicroRNAs in Psoriasis: A Systematic Review of the Literature. *Medicine (Baltimore)* **2015**, *94*, e2030. [CrossRef] [PubMed]

8. Amarilyo, G.; La Cava, A. miRNA in systemic lupus erythematosus. *Clin. Immunol.* **2012**, *144*, 26–31. [CrossRef] [PubMed]

9. Sedivy, J.M.; Banumathy, G.; Adams, P.D. Aging by epigenetics—A consequence of chromatin damage? *Exp. Cell Res.* **2008**, *314*, 1909–1917. [CrossRef] [PubMed]

10. Deaton, A.M.; Bird, A. CpG islands and the regulation of transcription. *Genes Dev.* **2011**, *25*, 1010–1022. [CrossRef] [PubMed]

11. Santos-Rosa, H.; Schneider, R.; Bannister, A.J.; Sherriff, J.; Bernstein, B.E.; Emre, N.C.; Schreiber, S.L.; Mellor, J.; Kouzarides, T. Active genes are tri-methylated at K4 of histone H3. *Nature* **2002**, *419*, 407–411. [CrossRef] [PubMed]

12. Bernstein, B.E.; Kamal, M.; Lindblad-Toh, K.; Bekiranov, S.; Bailey, D.K.; Huebert, D.J.; McMahon, S.; Karlsson, E.K.; Kulbokas, E.J., 3rd; Gingeras, T.R.; et al. Genomic maps and comparative analysis of histone modifications in human and mouse. *Cell* **2005**, *120*, 169–181. [CrossRef] [PubMed]

13. Li, Z.; Rana, T.M. Therapeutic targeting of microRNAs: Current status and future challenges. *Nat. Rev. Drug Discov.* **2014**, *13*, 622–638. [CrossRef] [PubMed]

14. Reddy, D.; Siegel, C.A.; Sands, B.E.; Kane, S. Possible association between isotretinoin and inflammatory bowel disease. *Am. J. Gastroenterol.* **2006**, *101*, 1569–1573. [CrossRef] [PubMed]

15. Shale, M.; Kaplan, G.G.; Panaccione, R.; Ghosh, S. Isotretinoin and intestinal inflammation: What gastroenterologists need to know. *Gut* **2009**, *58*, 737–741. [CrossRef] [PubMed]

16. Crockett, S.D.; Porter, C.Q.; Martin, C.F.; Sandler, R.S.; Kappelman, M.D. Isotretinoin use and the risk of inflammatory bowel disease: A case-control study. *Am. J. Gastroenterol.* **2010**, *105*, 1986–1993. [CrossRef] [PubMed]

17. Bernstein, C.N.; Nugent, Z.; Longobardi, T.; Blanchard, J.F. Isotretinoin is not associated with inflammatory bowel disease: A population-based case-control study. *Am. J. Gastroenterol.* **2009**, *104*, 2774–2778. [CrossRef] [PubMed]

18. Popescu, C.M.; Popescu, R. Isotretinoin therapy and inflammatory bowel disease. *Arch. Dermatol.* **2011**, *147*, 724–729. [CrossRef] [PubMed]

19. Thakrar, B.T.; Robinson, N.J. Isotretinoin use and the risk of inflammatory bowel disease. *Am. J. Gastroenterol.* **2011**, *106*, 1000–1002. [CrossRef] [PubMed]

20. Frey-Wagner, I.; Fischbeck, A.; Cee, A.; Leonardi, I.; Gruber, S.; Becker, E.; Atrott, K.; Lang, S.; Rogler, G. Effects of retinoids in mouse models of colitis: Benefit or danger to the gastrointestinal tract? *Inflamm. Bowel Dis.* **2013**, *19*, 2356–2365. [CrossRef] [PubMed]

21. Wojtal, K.A.; Wolfram, L.; Frey-Wagner, I.; Lang, S.; Scharl, M.; Vavricka, S.R.; Rogler, G. The effects of vitamin A on cells of innate immunity in vitro. *Toxicol. In Vitro* **2013**, *27*, 1525–1532. [CrossRef] [PubMed]

22. Margolis, D.J.; Fanelli, M.; Hoffstad, O.; Lewis, J.D. Potential association between the oral tetracycline class of antimicrobials used to treat acne and inflammatory bowel disease. *Am. J. Gastroenterol.* **2010**, *105*, 2610–2616. [CrossRef] [PubMed]

23. Williams, H.C.; Dellavalle, R.P.; Garner, S. Acne vulgaris. *Lancet* **2012**, *379*, 361–372. [CrossRef]

24. Shaw, S.Y.; Blanchard, J.F.; Bernstein, C.N. Association between the use of antibiotics in the first year of life and pediatric inflammatory bowel disease. *Am. J. Gastroenterol.* **2010**, *105*, 2687–2692. [CrossRef] [PubMed]

25. Hviid, A.; Svanstrom, H.; Frisch, M. Antibiotic use and inflammatory bowel diseases in childhood. *Gut* **2011**, *60*, 49–54. [CrossRef] [PubMed]

26. Shaw, S.Y.; Blanchard, J.F.; Bernstein, C.N. Association between the use of antibiotics and new diagnoses of Crohn's disease and ulcerative colitis. *Am. J. Gastroenterol.* **2011**, *106*, 2133–2142. [CrossRef] [PubMed]

27. Ungaro, R.; Bernstein, C.N.; Gearry, R.; Hviid, A.; Kolho, K.L.; Kronman, M.P.; Shaw, S.; Van Kruiningen, H.; Colombel, J.F.; Atreja, A. Antibiotics associated with increased risk of new-onset Crohn's disease but not ulcerative colitis: A meta-analysis. *Am. J. Gastroenterol.* **2014**, *109*, 1728–1738. [CrossRef] [PubMed]

28. Becker, E.; Bengs, S.; Aluri, S.; Opitz, L.; Atrott, K.; Stanzel, C.; Castro, P.A.; Rogler, G.; Frey-Wagner, I. Doxycycline, metronidazole and isotretinoin: Do they modify microRNA/mRNA expression profiles and function in murine T-cells? *Sci. Rep.* **2016**, *6*, 37082. [CrossRef] [PubMed]

29. Shin, C.; Nam, J.W.; Farh, K.K.; Chiang, H.R.; Shkumatava, A.; Bartel, D.P. Expanding the microRNA targeting code: functional sites with centered pairing. *Mol. Cell* **2010**, *38*, 789–802. [CrossRef] [PubMed]

30. Lewis, B.P.; Burge, C.B.; Bartel, D.P. Conserved seed pairing, often flanked by adenosines, indicates that thousands of human genes are microRNA targets. *Cell* **2005**, *120*, 15–20. [CrossRef] [PubMed]

31. Shivdasani, R.A. MicroRNAs: Regulators of gene expression and cell differentiation. *Blood* **2006**, *108*, 3646–3653. [CrossRef] [PubMed]

32. Smith, Z.D.; Meissner, A. DNA methylation: Roles in mammalian development. *Nat. Rev. Genet.* **2013**, *14*, 204–220. [CrossRef] [PubMed]

33. Ventham, N.T.; Kennedy, N.A.; Nimmo, E.R.; Satsangi, J. Beyond gene discovery in inflammatory bowel disease: The emerging role of epigenetics. *Gastroenterology* **2013**, *145*, 293–308. [CrossRef] [PubMed]

34. Karatzas, P.S.; Gazouli, M.; Safioleas, M.; Mantzaris, G.J. DNA methylation changes in inflammatory bowel disease. *Ann. Gastroenterol.* **2014**, *27*, 125–132. [PubMed]

35. Tschurtschenthaler, M.; Kachroo, P.; Heinsen, F.A.; Adolph, T.E.; Ruhlemann, M.C.; Klughammer, J.; Offner, F.A.; Ammerpohl, O.; Krueger, F.; Smallwood, S.; et al. Paternal chronic colitis causes epigenetic inheritance of susceptibility to colitis. *Sci. Rep.* **2016**, *6*, 31640. [CrossRef] [PubMed]

36. Low, D.; Mizoguchi, A.; Mizoguchi, E. DNA methylation in inflammatory bowel disease and beyond. *World J. Gastroenterol.* **2013**, *19*, 5238–5249. [CrossRef] [PubMed]

37. Harris, R.A.; Wang, T.; Coarfa, C.; Nagarajan, R.P.; Hong, C.; Downey, S.L.; Johnson, B.E.; Fouse, S.D.; Delaney, A.; Zhao, Y.; et al. Comparison of sequencing-based methods to profile DNA methylation and identification of monoallelic epigenetic modifications. *Nat. Biotechnol.* **2010**, *28*, 1097–1105. [CrossRef] [PubMed]

38. Aberg, K.A.; Xie, L.; Chan, R.F.; Zhao, M.; Pandey, A.K.; Kumar, G.; Clark, S.L.; van den Oord, E.J. Evaluation of Methyl-Binding Domain Based Enrichment Approaches Revisited. *PLoS ONE* **2015**, *10*, e0132205. [CrossRef] [PubMed]

39. Pasquinelli, A.E. MicroRNAs and their targets: Recognition, regulation and an emerging reciprocal relationship. *Nat. Rev. Genet.* **2012**, *13*, 271–282. [CrossRef] [PubMed]

40. Pedrotti, L.P.; Barrios, B.E.; Maccio-Maretto, L.; Bento, A.F.; Sena, A.A.; Rodriguez-Galan, M.C.; Calixto, J.B.; Correa, S.G. Systemic IL-12 burst expands intestinal T-lymphocyte subsets bearing the $\alpha_4\beta7$ integrin in mice. *Eur. J. Immunol.* **2016**, *46*, 70–80. [CrossRef] [PubMed]

41. Henriques, C.M.; Rino, J.; Nibbs, R.J.; Graham, G.J.; Barata, J.T. IL-7 induces rapid clathrin-mediated internalization and JAK3-dependent degradation of IL-7Rα in T cells. *Blood* **2010**, *115*, 3269–3277. [CrossRef] [PubMed]

42. Faller, E.M.; Ghazawi, F.M.; Cavar, M.; MacPherson, P.A. IL-7 induces clathrin-mediated endocytosis of CD127 and subsequent degradation by the proteasome in primary human CD8 T cells. *Immunol. Cell Biol.* **2016**, *94*, 196–207. [CrossRef] [PubMed]

43.   Lin, Z.; Hegarty, J.P.; Yu, W.; Cappel, J.A.; Chen, X.; Faber, P.W.; Wang, Y.; Poritz, L.S.; Fan, J.B.; Koltun, W.A. Identification of disease-associated DNA methylation in B cells from Crohn's disease and ulcerative colitis patients. *Dig. Dis. Sci.* **2012**, *57*, 3145–3153. [CrossRef] [PubMed]

44.   Liu, J.Z.; van Sommeren, S.; Huang, H.; Ng, S.C.; Alberts, R.; Takahashi, A.; Ripke, S.; Lee, J.C.; Jostins, L.; Shah, T.; et al. Association analyses identify 38 susceptibility loci for inflammatory bowel disease and highlight shared genetic risk across populations. *Nat. Genet.* **2015**, *47*, 979–986. [CrossRef] [PubMed]

45.   Matsuzaki, K.; Tsuzuki, Y.; Matsunaga, H.; Inoue, T.; Miyazaki, J.; Hokari, R.; Okada, Y.; Kawaguchi, A.; Nagao, S.; Itoh, K.; et al. In vivo demonstration of T lymphocyte migration and amelioration of ileitis in intestinal mucosa of SAMP1/Yit mice by the inhibition of MAdCAM-1. *Clin. Exp. Immunol.* **2005**, *140*, 22–31. [CrossRef] [PubMed]

46.   Soler, D.; Chapman, T.; Yang, L.L.; Wyant, T.; Egan, R.; Fedyk, E.R. The binding specificity and selective antagonism of vedolizumab, an anti-$\alpha_4\beta7$ integrin therapeutic antibody in development for inflammatory bowel diseases. *J. Pharmacol. Exp. Ther.* **2009**, *330*, 864–875. [CrossRef] [PubMed]

47.   Coombes, J.L.; Siddiqui, K.R.; Arancibia-Carcamo, C.V.; Hall, J.; Sun, C.M.; Belkaid, Y.; Powrie, F. A functionally specialized population of mucosal CD103+ DCs induces Foxp3+ regulatory T cells via a TGF-β and retinoic acid-dependent mechanism. *J. Exp. Med.* **2007**, *204*, 1757–1764. [CrossRef] [PubMed]

48.   Wittmann, A.; Bron, P.A.; van Svam, I.I.; Kleerebezem, M.; Adam, P.; Gronbach, K.; Menz, S.; Flade, I.; Bender, A.; Schafer, A.; et al. TLR signaling-induced CD103-expressing cells protect against intestinal inflammation. *Inflamm. Bowel Dis.* **2015**, *21*, 507–519. [CrossRef] [PubMed]

49.   D'Agostino, P.; Arcoleo, F.; Barbera, C.; Di Bella, G.; La Rosa, M.; Misiano, G.; Milano, S.; Brai, M.; Cammarata, G.; Feo, S.; et al. Tetracycline inhibits the nitric oxide synthase activity induced by endotoxin in cultured murine macrophages. *Eur. J. Pharmacol.* **1998**, *346*, 283–290. [CrossRef]

50.   Griffin, M.O.; Fricovsky, E.; Ceballos, G.; Villarreal, F. Tetracyclines: A pleitropic family of compounds with promising therapeutic properties. Review of the literature. *Am. J. Physiol. Cell Physiol.* **2010**, *299*, C539–C548. [CrossRef]

51.   Becker, E.; Schmidt, T.S.B.; Bengs, S.; Poveda, L.; Opitz, L.; Atrott, K.; Stanzel, C.; Biedermann, L.; Rehman, A.; Jonas, D.; et al. Effects of oral antibiotics and isotretinoin on the murine gut microbiota. *Int. J. Antimicrob. Agents* **2017**, *50*, 342–351. [CrossRef] [PubMed]

52.   Nakanishi, Y.; Sato, T.; Ohteki, T. Commensal Gram-positive bacteria initiates colitis by inducing monocyte/macrophage mobilization. *Mucosal Immunol.* **2015**, *8*, 152–160. [CrossRef] [PubMed]

53.   Robinson, M.D.; McCarthy, D.J.; Smyth, G.K. edgeR: A bioconductor package for differential expression analysis of digital gene expression data. *Bioinformatics* **2010**, *26*, 139–140. [CrossRef] [PubMed]

54.   Chen, C.J.; Servant, N.; Toedling, J.; Sarazin, A.; Marchais, A.; Duvernois-Berthet, E.; Cognat, V.; Colot, V.; Voinnet, O.; Heard, E.; et al. ncPRO-seq: A tool for annotation and profiling of ncRNAs in sRNA-seq data. *Bioinformatics* **2012**, *28*, 3147–3149. [CrossRef] [PubMed]

55.   Langmead, B.; Salzberg, S.L. Fast gapped-read alignment with Bowtie 2. *Nat. Methods* **2012**, *9*, 357–359. [CrossRef] [PubMed]

56.   Wu, H.; Caffo, B.; Jaffee, H.A.; Irizarry, R.A.; Feinberg, A.P. Redefining CpG islands using hidden Markov models. *Biostatistics* **2010**, *11*, 499–514. [CrossRef] [PubMed]